ELECTRON TRANSPORT PROPERTIES OF DSSC BASED ON ZNO NANOWIRE ARRAYS

Nuraje N., assistant professor, PhD*;
Ilyassov B.R., PhD candidate**; Ibrayev N.Kh., d.pf.-m.s., professor**;
Abzhanova D.B., master**
*Texas Tech University, Department of Chemical Engineering, Box 43121, Lubbock, TX 79409-3121, USA;
**Y.A. Buketov Karaganda State University
Karaganda, the Republic of Kazakhstan

Abstract. ZnO nanorod arrays were synthesized by hydrothermal method for 8, 10, and 12 hours. The array synthesized for 10h had the highest surface area and aspect ratio, and DSSC based on the 10h nanorod array revealed the best photovoltaic performance. The electron transport properties of DSSC based on the ZnO nanowire arrays were investigated by Electrochemical Impedance Spectroscopy (EIS).

Introduction

Dye sensitized solar cells (DSSCs) based on nanostructured metal oxides attract much attention of researchers in the recent years [1-3]. Preparation technologies of DSSCs are much easier and cheaper than one of solar cells based on p-n junction [1-3]. The efficiency of DSSCs has reached a value of more than 10% [4-5], and the efficiency of organic-inorganic perovskite solar cells which are also based on metal oxides has exceeded 15% [6].

One of the key components of the DSSCs is a metal oxide semiconductor photoelectrode which performs a double function: (1) It is a scaffold with a large specific surface needed for the dye loading, and (2) at the same time it is an electron transport material [1]. Morphology and defect density of the metal oxide determine its specific surface and its electron transport properties, respectively, and also influence on electron recombination in DSSCs. Nanostructured TiO_2 currently is being studied as photoelectrode of DSSCs most of all. High efficient DSSCs have been reached on TiO_2.

ZnO nanostructures are alternative material as a photoelectrode of DSSC. The bandgap and the conduction band edge position of ZnO is approximately the same as that of TiO_2. The first advantage of ZnO over TiO_2 is a large variety of nanocrystals with different morphology that have sufficiently large specific surface area. These ZnO nanocrystals can be obtained by solution processable methods [7-10]. The second is the electron mobility in ZnO, at least in single crystals, by an order of magnitude is greater than that of TiO_2 (anatase) [11-14]. However so far, the efficiency of DSSCs based on ZnO nanostructures is lower than one based on TiO_2. The efficiency of DSSCs based on multilayer assembly of ZnO nanowire arrays has reached 7% [15].

Several reports suggest that dye adsorption is the major problem in ZnO DSSCs [16-18]. Cells with high dye loading tend to be inefficient, whereas cells with lower dye loading show good quantum efficiencies. These problems are mainly related to the high acidity of the carboxylic acid binding groups of the dyes that can lead to dissolution of ZnO and precipitation of dye-Zn^{2+} complexes, leading to a poor overall electron injection efficiency of the dye [18].

According to the report [19], the majority of studies regarding ZnO DSSCs have been focused on two main aspects: (1) using the ease of preparing one-dimensional ZnO nanostructures with attractive transport properties and (2) searching for suitable dyes for ZnO. However, in comparison with TiO_2, less detailed studies of electron transport and recombination have been carried out on DSSCs based on ZnO nanostructures.

Vertically aligned ZnO nanowire arrays have recently attracted considerable interest because of their one-dimensional structure and unique properties. In the field of energy conversion, nanowire DSSCs have been fabricated based on the fast electron transport in single crystalline ZnO nanowires. The majority of studies regarding ZnO nanowires for DSSC have been concentrated on preparing nanowires with the high aspect ratio and density on a substrate that gives the high surface area of nanowires. However, there are no researches related to an effect of morphology of ZnO nanowires on electron transport properties of DSSCs.

In this paper, we studied the effect of morphology of ZnO nanowire arrays on the photovoltaic and electron transport properties of DSSC. ZnO nanowire arrays were synthesized by hydrothermal methods. Electron transport properties of DSSC based on the ZnO nanowire arrays were investigated by Electrochemical Impedance Spectroscopy (EIS).

Experimental procedure

1.1. Preparation of ZnO nanowire arrays

Preparation of ZnO seed layers. ZnO seed layers were prepared by the sol-gel spin coating fabrication process [30]. Zinc acetate dehydrate [$(Zn(CH_3COO)_2 \cdot 2H_2O$, Sigma Aldrich)] was dissolved in the mixed solution of monoethanolamine (C_2H_7NO, Sigma-Aldrich) and isopropyl alcohol. The concentrations of both zinc acetate dehydrate and monoethanolamine in the resulting solution are 0.5 M. The coating solution was spin-coated onto ITO substrates at 3000 rpm for several times. The ITO substrates were subsequently annealed at 400°C in air for 30 min in order to convert zinc acetate to ZnO.

Hydrothermal deposition. ZnO nanowires were prepared by hydrothermal deposition [21]. ZnO nanowires were grown by placing vertically the ZnO-seeded ITO substrates in solutions with 25 mM $Zn(NO_3)_2$ (Sigma-Aldrich) and 25 mM hexamethylenetetramine ($C_6H_{12}N_4$, Sigma-Aldrich) at 90°C for 8, 10 and 12 hours. In order to obtain a constant nanowire array growth rate, the solutions were refreshed during the reaction period (solution turnover time 2 h). Subsequently, the substrates were washed with water/ethanol and annealed at 400°C for 30 min to remove any residual organics.

1.2. Assembly of DSSC

The ZnO-based photoanodes, each with an active surface area of 0.2 cm^2, were dyed by immersing them in a dry ethanol solution containing 0.5 mM of N719 (Solaronix) at 50 °C for 1 h. An ITO substrate coated with Pt was used as the counter electrode. Pt coat was prepared by electrodeposition methods on ITO that can be found elsewhere [22, 23] The DSSC was fabricated by placing the Pt-coated counter electrode over the dyed ZnO-based photoanode separated by a 25 μm thick thermoplastic sealing spacer (Meltonix 1170-25, Solaronix). The internal space of cell was filled with a high stable liquid electrolyte, Iodolyte Z-150 (Solaronix; Redox couple: iodide/tri-iodide; redox concentration: 150 mM; additives: ionic liquid, alkylbenzimidazole, thiocyanate; solvent: 3-methoxypropionitrile).

1.3. Measurements

The surface morphology of ZnO nanowire arrays was characterized on a field-emission scanning electron microscope (FESEM MIRA-3, Tescan). The photocurrent-voltage characteristics were measured using a Source Meter instruments (Keithley 2400) by irradiating with simulated solar light, that is, AM 1.5 100 mW/cm^2 (PET PHOTO Emission TECH., INC). The cell active area was 0.2 cm^2. The impedance of the cells was measured by using an impedance meter (Z-500PRO, Elins). All impedance measurements were performed under a bias light illumination of 100 mW/cm^2 from a simulated solar light (PET PHOTO Emission TECH., INC) at open circuit condition. Impedance measurement of cells was recorded in a frequency range from 0.05 Hz to 200 kHz with an ac amplitude of 10 mV.

Result and discussion

Figure 1 shows the SEM top view images of ZnO nanowire (NR) arrays synthesized for 8, 10, and 12 hours. Table 1 shows morphology parameters of NW arrays (NW density, diameter, length, and aspect ratio) calculated from the data of SEM. As shown in Figure 1 and table 1, the NW average diameter and length increase with the increasing of reaction time while NW density (number per cm^2 of projected surface area) decreases. On the basis of these calculated parameters, the surface area of the NW arrays was approximately evaluated (see table 1). At the beginning the NW surface area increases from 61 to 81 cm^2 when the reaction time is increased from 8 to 10 h, respectively, and further at 12 h it decreases to 65 cm^2. The aspect ratio (diameter/length) also has a maximum value for the 10 h NW array.

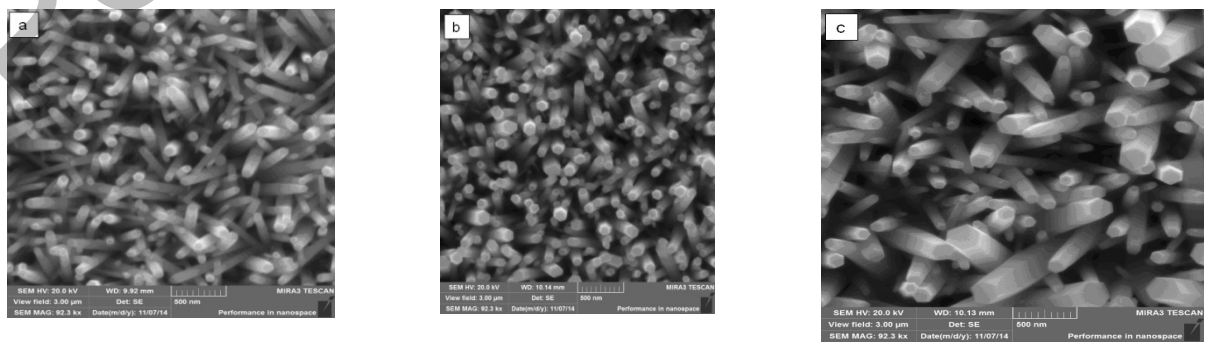

Figure 1. The SEM top view images of ZnO nanowire arrays synthesized for 8 (a), 10 (b), and 12h (c).

Table 1. Morphology parameters of ZnO nanowire array synthesized for 8, 10, and 12 h.

Reaction time, h	Nanorod density	Average nanorod diameter (R), nm	Average nanorod length (L), μm	R/L	Surface area of nanorod array, cm^2
8	$503 \cdot 10^7$	92	2.1	$4.38 \cdot 10^{-2}$	61
10	$295 \cdot 10^7$	151	2.9	$5.20 \cdot 10^{-2}$	81
12	$215 \cdot 10^7$	156	3.1	$5.03 \cdot 10^{-2}$	65

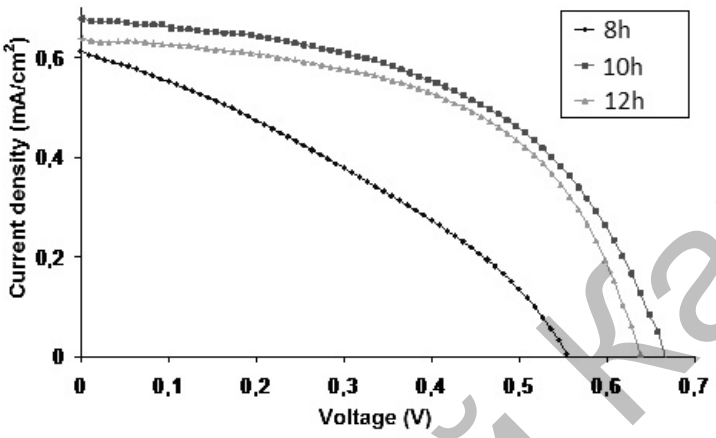

Figure 2. Current-voltage characteristics of DSSCs based on ZnO NW arrays synthesized for 8, 10, and 12 h.

Table 2. Photovoltaic performances and electron transport properties of DSSCs based on ZnO NW arrays synthesized for 8, 10, and 12 h.

Reaction time	J_{sc}, мкА/см^2	U_{oc}	FF	η, %	R_w, Ом	R_k, Ом	R_k/R_w	k_{eff}, c^{-1}	τ_{eff}, мс	D_{eff}, см^2/с
8h	610	0.55	0.42	0.11	9.1	130	14	16	62	$0.99 \cdot 10^{-05}$
10h	680	0.66	0.52	0.25	8	89	11	36	28	$3.34 \cdot 10^{-05}$
12h	629	0.63	0.55	0.22	5	65	13	71	14	$8.92 \cdot 10^{-05}$

The current-voltage characteristic of DSSCs based on ZnO NW arrays synthesized for 8, 10, and 12 h. are shown in figure 2 and their photovoltaic performances are listed in table 2. The cell based on the array grown for 10h has revealed the highest conversion efficiency, short circuit current density, and open circuit photovoltage. This result confirms that the 10h grown array has the highest surface area.

Effect of nanowire morphology parameters on electron transport properties of the DSSCs were investigated using Electrochemical Impedance Spectroscopy (EIS). Figure 3 represents the Nyquist plots of the impedance data of the cells operated in the open circuit under the standard illumination. According to the diffusion-recombination model [24], a suggested equivalent circuit representing the DSSCs based on NW array shown in the figure 4 is employed to fit the impedance spectra for extracting the impedance of the nanowires and the nanowires/electrolyte interface portions. The fitted results are the solid lines shown in the Figure 3. Estimation of the electron transport parameters in the nanowires and electron transfer parameters on the nanowire/electrolyte interface of the cells was conducted from the Nyquist plots of the nanowire and the nanowire/electrolyte interface portions according to the procedure demonstrated by Adachi et al. [25]. The electron transport resistance in NWs ($R_w = r_w L$, as shown in the equivalent circuit and L is the thickness of the anode), charge-transfer resistance related to recombination of an electron ($R_k = r_k/L$), first-order reaction rate constant for electrons being lost (k_{eff}), lifetime of an electron in ZnO NWs (τ) estimated from the impedance analyses are also listed in Table 1.

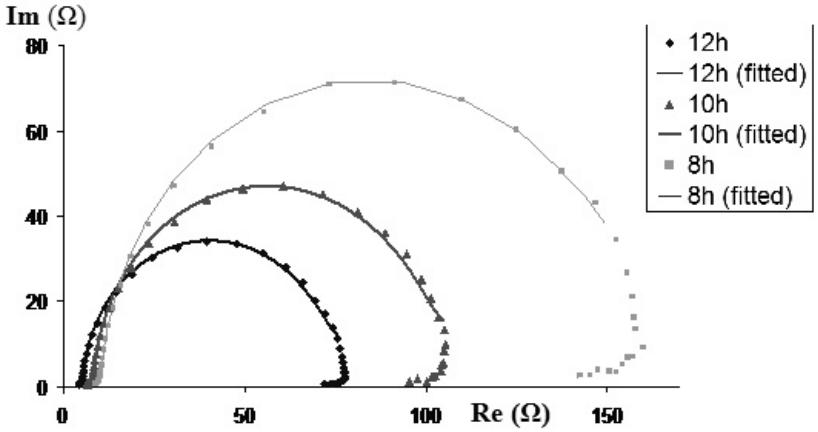

Figure 3. Nyquist plots of the impedance data of DSSCs based on ZnO NW arrays synthesized for 8, 10, and 12 h. The solid lines are the fitting results based on the equivalent circuit model shown in the figure 4.

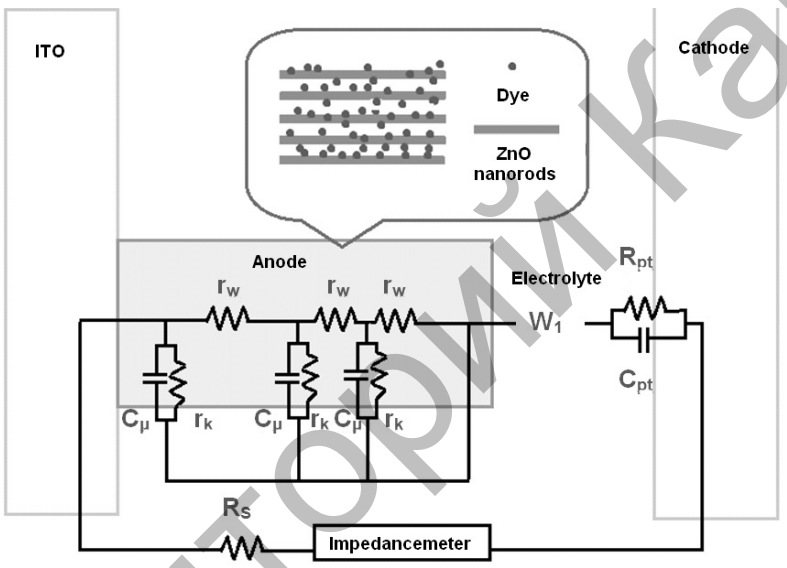

Figure 4. The equivalent circuit model of DSSCs based on NW arrays, where $C_\mu(=c_\mu L)$ is the chemical capacitance, R_s is a total series resistance for the transport resistance of ITO and all resistances out of the cell, W_1 is the impedance of diffusion of redox species in the electrolyte, and R_{Pt} and C_{Pt} are the charge transfer resistance and the interfacial capacitance at the counter electrode/ electrolyte interface, respectively [26].

As shown in Table 1, when the reaction time of NW synthesis is increased from 8 to 12 h, the electron transport resistance in NWs decreases, consequently, FF of cells improves. The electron recombination resistance and lifetime of an electron also decrease with increasing the reaction time. The latter indicates that with increasing the reaction time of NW synthesis recombination losses of electron intensify. It is can be due to increasing a defect density on NW surface. According to the diffusion and recombination model of the impedance of DSSC based on TiO_2 [27], that confirmed by the EIS, only trapped photoinjected elections on the semiconductor/electrolyte are lost by the recombination with electrolytes species I_{3-}.

Conclusion

In summary, ZnO nanowire arrays were synthesized by hydrothermal method for 8, 10, 12 hours. The arrays synthesized for 10h have the highest surface area and aspect ratio, and DSSC based on their revealed the best photovoltaic performance. According to the EIS date, with the increasing of reaction time of nanowire arrays from 8 to 12 h, the electron transport resistance, the electron recombination resistance and the electron lifetime in ZnO nanorods decrease. Decreasing the electron recombination resistance improves FF of cells while decreasing the electron recombination resistance and the electron deteriorates photovoltaic performance of DSSCs.

References:

[1] O'Regan B., Gräzel M. 1991. A low-cost, high-efficiency solar cell based on dye-sensitized colloidal TiO_2 films. *Nature.* **353**, 737–740.

[2] Kong F.-T., Dai S.-Y., Wang K.-J. 2013. Review of Recent Progress in Dye-Sensitized Solar Cells. *Adv. Opto Elect*. **75384**, 13.

[3] Hamann T. W., Jensen R. A., Martinson A. B. F., Ryswyk H. V., Hupp J. T. 2008. Advancing Beyond Current Generation Dye-Sensitized Solar Cells. *Energy Environ. Sci*., **1**, 66–78.

[4] Hagfeldt A., Grätzel M. 2000. Molecular Photovoltaics. *Acc. Chem. Res*. **33**, 269–277.

[5] Grätzel M. 2001. Photoelectrochemical cells. *Nature*. **414**, 338–44.

[6] Burschka J., Pellet N., Moon S. J., Humphry-baker R., Gao P., Nazeeruddin M. K., Grätzel M. 2013. Sequential deposition as a route to high-performance perovskite-sensitized solar cells. *Nature*. **499**, 316–9.

[7] Baruah S., Dutta J. 2009. Hydrothermal growth of ZnO nanostructures. *Sci. Technol. Adv. Mater*. **10,** 18.

[8] Lamia Z. 2010. Sol–gel-deposited ZnO thin films. *Materials Science and Engineering B*. **174**, 18–30.

[9] Skompska M., Zarebska K. 2014. Electrodeposition of ZnO Nanorod Arrays on Transparent Conducting Substrates. *Electrochimica Acta*. **127**, 467–488.

[10] Chen H., Zhu L., Liu H., Li W. 2013. Effects of preparing conditions on the nanostructures electrodeposited from the $Zn(NO_3)_2$ electrolyte containing KCl. *Thin Solid Films*. **534**, 205–213.

[11] Law M., Greene L.E., Yang P. 2005. Nanowire dye-sensitized solar cells. *Nature Materials*. **4**, 455–459.

[12] Gao Y., Nagai M., Chang T.-C., Shyue J. 2007. Solution-Derived ZnO Nanowire Array Film as Photoelectrode in Dye-Sensitized Solar Cells. *Crystal Growth and Design*. **7**, 2467–2471.

[13] Kaidashev E. M., Lorenz M., von Wenckstern H., Rahm A., Semmelhack H.-C., Han K.-H., Benndorf G., Bundesmann C., Hochmuth H., Grundmann M. 2003. High electron mobility of epitaxial ZnO thin films on c-plane sapphire grown by multistep pulsed-laser deposition. *Applied Physics Letters*. **82**, 3901–3903.

[14] Hendry E., Koeberg M., O'Regan B., Bonn M. 2006. Local field effects on electron transport in nanostructured TiO_2 revealed by terahertz spectroscopy. *Nano Letters*. **6**, 755–759.

[15] Xu C., Wu J., Desai U. V., Gao D. 2011. Multilayer Assembly of Nanowire Arrays for Dye-Sensitized Solar Cells. *J. Am. Chem. Soc*. **133**, 8122–8125.

[16] Gao Y., Nagai M., Chang T.-C., Shyue J. 2007. Solution-Derived ZnO Nanowire Array Film as Photoelectrode in Dye-Sensitized Solar Cells. *Crystal Growth and Design*. **7**, 2467–2471.

[17] Kaidashev E. M., Lorenz M., von Wenckstern H., Rahm A., Semmelhack H.-C., Han K.-H., Benndorf G., Bundesmann C., Hochmuth H., Grundmann M. 2003. High electron mobility of epitaxial ZnO thin films on c-plane sapphire grown by multistep pulsed-laser deposition. *Applied Physics Letters*. **82**, 3901–3903.

[18] Hendry E., Koeberg M., O'Regan B., Bonn M. 2006. Local field effects on electron transport in nanostructured TiO_2 revealed by terahertz spectroscopy. *Nano Letters*. **6**, 755–759.

[19] Guill E., Peter L. M., Anta J. A. Electron Transport and Recombination in ZnO-Based Dye-Sensitized Solar Cells. *E. J. Phys. Chem. C*. **115**, 22622–32.

[20] Kamaruddin S.A., Chan K., Yow H., Sahdan M.Z., Saim H., Knipp D. 2011. Zinc oxide films prepared by sol-gel spin coating technique. *Applied Physics A*. **104**, 263–268.

[21] Baruah S., Dutta J. 2009. Hydrothermal growth of ZnO nanostructures. Sci. Technol. *Adv. Mater*. **10**, 18.

[22] Lee K.S., Lee H.K., Wang D.H., Park N., Lee J.Y., Park O., Park J.H. 2010. Dye-sensitized solar cells with Pt- and TCO-free counter electrodes. *Chem. Commun*. **46**, 4505–4507.

[23] Gao Y., Chu L., Wu M., Wang L., Guo W., Ma T. 2012. Improvement of adhesion of Pt-free counter electrodes for low-cost dye-sensitized solar cells. *Journal of Photochemistry and Photobiology A: Chemistry*. **245**, 66–71.

[24] Bisquert J. 2002. Theory of the Impedance of Electron Diffusion and Recombination in a Thin Layer. *J. Phys. Chem. B*. **106**, 325–333.

[25] Adachi M., Sakamoto M., Jiu J., Ogata Y., Isoda S. 2006. Determination of Parameters of Electron Transport in Dye-Sensitized Solar Cells Using Electrochemical Impedance Spectroscopy. *J. Phys. Chem. B*. **110**, 13872–80.

[26] Wu J., Chen G., Yang H., Ku C., Lai J.-Y. 2007. Effects of dye adsorption on the electron transport properties in ZnO-nanowire dye sensitized solar cells. *Applied physics letters*. **90**, 2131091–3.

[27] Kern R., Sastrawan R., Ferber J., Stangl R., Luther J. 2002. Modeling and interpretation of electrical impedance spectra of dye solar cells operated under open-circuit conditions. *Electrochimica Acta*. **47**, 4213–4225.